

Optimum Approach Velocity for Twin Merging of Autonomous POD Vehicles

Osama M. Al-Habahbeh and Romil S. Al-Adwan

Mechatronics Engineering Department, School of Engineering, the University of Jordan, Amman, Jordan

Email: o.habahbeh@ju.edu.jo, romil.aladwan@ju.edu.jo

Abstract—Autonomous vehicles (AV) have gained ground in recent years. However, they still use the principles of traditional vehicles in terms of design and operation. This work proposes an adaptive transportation system based on autonomous POD vehicles, and investigates a major aspect of its operation. The PODs used in the proposed system can be considered a variant version of existing autonomous PODs. However, their unique design and concept of operation enable them to operate more efficiently than existing PODs. The proposed system involves docking and undocking of these PODs based on passengers' demands. However, during the merging process, undesired collisions could happen due to unforeseen conditions. If the approach speed is high enough, it could induce damage to the vehicles. This work investigates some possible scenarios of the potential collisions that could happen between these PODs during the merging process. Based on these scenarios, the allowed safe approach speeds are determined. These speeds can help in designing the operation of the proposed transportation system. Some of the variables considered in this work include; type of body material, shell thickness, impact speed, stress, deformation, and absorbed energy. The safe design merging speeds have been determined under different conditions.

Index Terms— Urban transportation, POD modular vehicle, Autonomous vehicle, Vehicle merging, Approach velocity, FEM analysis, Vehicle impact

I. INTRODUCTION

In recent years, what was considered science fiction in the eighties has become a reality. The advent of autonomous systems is gaining momentum and passenger vehicles are no exception. Autonomous vehicles (AVs) are now disrupting the transportation industry. Many of these vehicles have the same size as regular passenger cars, while some of them have only one seat. The latter category is often referred to as POD. Researchers have worked to advance the design of AVs, such as He et al. [1] who proposed a novel emergency steering control strategy based on hierarchical control architecture consisting of a decision-making layer and motion control layer. A novel motion controller for automated vehicles is presented by Xia et al. [2] which offers smaller steady-state errors and faster convergence speed.

The idea of merging vehicles was considered by researchers and designers. Merging vehicles and separating them enables upsizing and downsizing of the vehicle so as to accommodate a given number of

passengers. However, most probably, there will still be one or more vacant seats; this work proposes a solution to this issue which will be discussed later. Another benefit of merging vehicles is saving energy; imagine two vehicles driving comfortably on a level or down-sloped road. If these vehicles are joined, then one of their engines can be switched off. One more benefit of merging vehicles is that all passengers will reach the destination at the same time. Moreover, once the passengers are onboard, they can interact face-to-face. Some patents [3-9] have shown that PODs can merge and separate during their operation in response to demand. Operating Strategies for a new modular electric autonomous vehicle were presented by Ulrich et al. [10]; the vehicle consists of a drive unit and an interchangeable capsule. However, even though it is a sound idea, the capsule replacement process requires extra equipment, which makes it impractical. A platooning-control strategy for a fleet of Autonomous and Connected Trucks (ACTs) was developed by Gungor et al. [11]; this is an example of connecting cars for the purpose of reaching the destination simultaneously as well as reducing energy consumption. An experimental study of Denial of Service (DoS) attacks against Platoon of smart vehicles was carried out by Malik et al. [12].

During the vehicles' merging process, minor collisions could happen. Vehicle crashworthiness have received considerable attention in the literature. An extensive literature survey pertaining to the topic of crash box was conducted by Abdullah et al. [13]. Front rails were designed by Li et al. [14] to improve the crash performance of vehicle and reduce its structural mass using finite element analysis. A collaborative optimization process using optimal Latin hypercube design and response surface methodology was proposed by Liu et al. [15] to improve the vehicle crashworthiness in the frontal impacts. Munyazikwiye et al. [16] investigated whether a simple piecewise Lumped Parameter Model can serve as an accurate crash modeling tool. Yu et al. [17] applied a series of tailor rolled blank (TRB) structures to the front-end components of pure electric vehicle (PEV) for the design optimization of vehicle crashworthiness and lightweight. A multi-objective design approach with accelerated methodology was developed by Oztürk et al. [18] for a B-pillar (side door pillar) in which the intrusion velocity was decreased and the crash energy absorbed. The feasibility

of designing a honeycomb-like crash-box, as a cellular structure, was analyzed by Saenz-Dominguez et al. [19]. A multi-material design for a vehicle body considering both crashworthiness safety and social effects was developed by Chen et al. [20]. A hybrid design approach was introduced by Yusof et al. [21] to develop a conceptual design of oil palm polymer composite automotive crash box. Jin et al. [22] hypothesized that occupants will be better protected by using rotational seat to alter the occupant's orientation in accordance with the direction of impact. A data-driven artificial intelligence (AI) inverse problem solution for traffic collision reconstruction was successfully developed by Chen et al. [23].

Some studies have investigated impact problems for a variety of applications. They can provide insights for a better understanding of impact behavior. For example, the impact responses and residual properties of thin-walled carbon fiber-reinforced plastics tubes and aluminum (Al) tubes subjected to multiple axial impacts were explored by Liu et al. [24]. Öztürk et al. [25] evaluated the effects of failure criteria of steel B-pillar on the accuracy of impact simulation.

It is predicted that the deployment of AVs will decrease traffic accidents, because human error, which is considered the main reason of such accidents, will be eliminated. Nonetheless, AVs will still be subjected to other factors that may increase the possibility of getting involved in accidents. Some of these factors are due to vehicle's design, such as mechanical failures and sensor malfunction, while others are due to environmental factors, such as wind and frequency interference. Therefore, the study of crashworthiness of AV is equally important to their man-operated counterparts. An example of these studies is the work done by Zong et al. [26], who modeled impacts and driving characteristics of multiple AVs and RVs vehicles. A collision avoidance/mitigation system (CAMS) was proposed by Lee and Kum [27] to rapidly evaluate risks associated with all surrounding vehicles. Sequence of events data extracted from California automated vehicle (AV) collision reports were used by Song et al. [28] to investigate patterns and how they may be used to develop AV test scenarios. The characteristics and patterns of crashes involving connected and autonomous vehicles (CAV) were investigated by Xu et al. [29]. Adaptive Stress Testing (AST) in conjunction with encoding domain relevant information into the search procedure was implemented by Corso et al. [30] to identify useful failure scenarios of AV. The mechanism of AV-involved crashes was explored by Chen et al. [31]; they analyzed the impact of each feature on crash severity. Walker et al. [32] called the meteorological community to action and proactive engagement with the transportation community to enhance the safety of AV.

During vehicles' collision, the type of material of the vehicle's body plays a major role in the impact response. An example of past work studying this issue is the testing of composite materials with metallic reinforcements under dynamic axial loading by Dlugosch et al. [33]. A material model normally used for modelling fiber-reinforced

plastics was adopted by Müller et al. [34] to generate a material database for three hardwood species.

The current situation of autonomous vehicles is that most of them have multiple seats. However, single-seat POD vehicles are gaining a growing popularity due to their low energy consumption. On the other hand, the concept of modular AV is attracting more attention due the developments in communication technology and electronic processors. These modular AVs can join each other to form new bigger vehicles. They can also separate from each other in order to satisfy passengers' demand. In order to conduct the docking operation safely, it should be done at a reasonable speed. If the speed exceeds a certain limit, the resulting impact will be harmful to the vehicle's body. The exact value of the speed depends on the type of vehicle's body material. A fleet of modular AVs represents an adaptive transportation system. The modular AV considered in this work is a single-seat POD, as shown in Fig. 1. This work will focus on determining the optimum docking speed for two PODs in Twin configuration, as shown in Fig. 1. The possible reasons for impact during docking include wind, misalignment, sensor error, frequency interference etc. In order to perform the analysis, Finite element method (FEM) is used to simulate the Twin POD docking operation. The results of this work can help to design safer and more efficient operation of modular autonomous POD vehicles. Merging the two POD vehicles enables the following benefits:

- a) There will be no vacant seats, which is reflected in smaller vehicle size. This will save both energy and road space.
- b) In level and down-sloped roads, one of the motors can be switched-off so as to save energy.
- c) The passengers will reach the destination at the same time.
- d) The passengers can interact face-to-face, unlike virtual communication in other methods.

The proposed docking process can be done quickly, with minimal energy, while no extra equipment is needed. When the PODs merge normally, there is no collision, and the two matching hitching ports (as shown in Fig. 1) will join each other. However, without the determination of the proper speed, either higher or lower speed will be used. If lower speed is used, it will cause delays and inefficiencies in the process. On the other hand, if higher speed is used, it will cause damage in the structure of the vehicles. The safe docking speed is determined based on stress failure criterion of the POD's material. Other considered variables include shell thickness and energy absorbed. Different values of merging velocities are simulated and safe values are determined based on von mises stress failure criteria.

The operation of modular AVs was investigated by many researchers. However, most related work focused on platooning of vehicles, which means they are not physically connected as in this work, but they drive in one formulation. For examples; Liu et al. [35] optimized bus platooning to ensure dynamic capacity. A macro network scheduling model for electric modular vehicles for public transportation was proposed by Liu et al. [36]; where several modular cars form a formation. A bus consists of a

power module vehicle and a van module vehicle, and the van module vehicle needs to be towed by the power module vehicle to move. Chinmay et al. [37] explored the need to integrate the Network model and platooning system of Connected and Autonomous Vehicles (CAV) for highway environments.

Another aspect that has received considerable attention is planning the operation of modular AVs; Tian et al. [38] determined the optimal planning of transit services timing with modular vehicles. Lamotte et al. [39] found that allocating road capacity to bookable autonomous vehicles can reduce congestion costs. Ji et al. [40] proposed a strategy for flexible Modular Autonomous Vehicle (MAV) scheduling on transit routes to meet the time-varying passenger demand. Chen et al. [41] investigated the joint design of dispatch headway and vehicle capacity for one to one shuttle systems with oversaturated traffic to achieve the optimal tradeoff between general vehicle dispatching cost and customer waiting cost. A variable-capacity operation approach with modular transits for shared-use corridors was proposed by Shi et al. [42], in which both dispatch headway and vehicle capacity are decision variables. It is noted that the above researchers have focused on scheduling and timing of operation rather than physical docking of vehicles.

Adaptive transportation systems rely on a fleet of modular AVs that are responsive to passengers' demand. A direct transit network dispatch model for public transport EVs was developed by Liu et al. [43]. It enables scalable transportation capacity in order to meet changeable travel demands. They investigated two modes of operation; Intelligent connected mode and Traction mode. Tholen et al. [44] optimized the capacity of on-demand modules of passenger and parcel compartments onboard shared autonomous vehicle (SAV) used in urban transportation. Fielbaum [45] studied a feeder system that operates on-demand in a local zone. He showed that the autonomous vehicle technology (AVT) encourages larger fleets of smaller vehicles that follow more direct routes. When compared with the traditional technology (TT), the total savings induced by the AVT reach up to one third of TT's costs. A modular transit network system (MTNS) concept is proposed by Pei et al. [46] to overcome the mismatch between fixed vehicle capacity and spatially varying travel demand in traditional public transportation systems. In this work, the proposed PODs transportation system operates based on travel demand, similar to the above previous works. However, this work looks more closely at the joining process and performs a dynamic analysis to better plan the PODs' docking operation in terms of design, material and velocity.

II. METHODOLOGY AND SIMULATION MODEL

In order to simulate the docking process of the two POD vehicles, two FEM models of these POD vehicles must be built and simulated; the two autonomous PODs to be joined as a twin are shown in Fig. 1. The width of the POD is 1 m, the height is 1.5 m, and the length is 3 m. Each POD can comfortably accommodate a single passenger along with his belongings or shopping. The merging process will

be conducted by joining the hitching ports of both vehicles, as shown in Fig. 1. This vehicle is part of the proposed smart transportation system where the passenger orders a ride using a mobile app. A central control room finds the vehicle that is nearest to the customer and commands it to drive to the customer's location. The vehicle does exactly that, picks up the customer, drives the customer to his destination then drops him off at the planned location. After that the vehicle will wait for new instructions or probably the instructions could have been received while the passenger was still onboard.

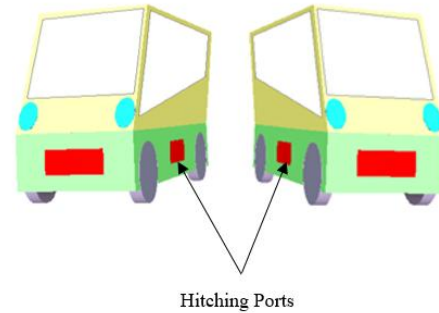


Figure 1. Front view of the two Autonomous PODs.

If two passengers order a vehicle, a corresponding number of PODs will drive to the passengers' location and merge together to form a twin vehicle, as shown in Fig. 2. The merging process will be done autonomously; when the two PODs want to merge in Twin configuration; one of them will be parking while the other one approaches it laterally. The important parameters in this operation include the approach velocity during merger, and the angle of alignment. If the approach velocity is small, the merging process will be slow, and after accumulating the lost times over the whole fleet and over a long period of operation, the loss of time (and earnings) will be high. On the other hand, if the approach velocity is high, the merging impact could cause damage in the PODs. Therefore, there is a need to determine an optimum value of approach velocity, where it is fast enough to maximize profit, while being slow enough to maintain safety. The back view of the two Autonomous PODs is shown in Fig. 2.

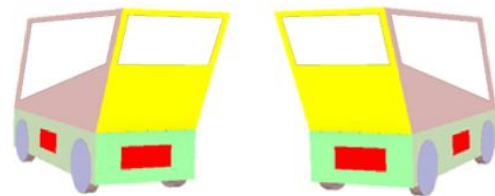


Figure 2. Back view of the two Autonomous PODs.

The geometric models of the POD vehicles shown in Fig. 1 and Fig. 2 will be used to simulate the merging process using FEM. If the merging process is performed at the right speed, no problem will occur. However, if the speed is too high, an impact will take place during merging. The body of the vehicle can be manufactured from different materials including metal alloys and composites. Various thicknesses of the POD's outer body will be investigated. Another possible variable is the impact angle. Different

impact velocities will be investigated in order to find the optimum approach velocity. In order to assess the possible damage due to impact, a failure criterion must be adopted. It will depend on the type of material used. The simulation process is performed using ANSYS™ software; where the procedure starts with developing geometric models of the two collided vehicles, as shown in Fig. 1 and Fig. 2. After that a FEM mesh of the two collided vehicles is generated. The collision loads are then applied and stresses and deformations are determined. Applying the principle of work and energy on the two PODs, we can write the energy balance during collision as shown in (1), [47].

$$(T_1 + T_2)_i + U_{i-f} = (T_1 + T_2)_f \quad (1)$$

where T_1 and T_2 are the kinetic energies of the first and second PODs, respectively. The subscripts i and f denote the initial state before collision and the final state after collision. U denotes the work done during collision, which equals the force in eqn. (1) times the deformation. Applying the impulse momentum theorem, we can write the corresponding equation as:

$$(m_1 v_1 + m_2 v_2)_i + \int_i^f F dt = (m_1 v_1 + m_2 v_2)_f \quad (2)$$

where m_1 and m_2 are the masses of POD₁ and POD₂, respectively, while v_1 and v_2 are the speeds of POD₁ and POD₂, respectively. Note that the impulse term represents the force of the moving POD's motor. Internal forces are reciprocated between the two PODs during collision. As a result of these forces, stress develops in the adjacent structures of the vehicles' bodies. As mentioned earlier, different materials of the vehicles' bodies are investigated. The properties of these materials are shown in Table I.

III. RESULTS AND DISCUSSION

The FEM models of the two PODs are used to simulate the merging scenario into twin configuration. After merging, the two vehicles will form a new bigger vehicle as shown in Fig. 3. The ideal case is when the merging is done accurately in terms of approach angle; that means the two merging PODs are perfectly parallel before and during attachment. In this case the impact angle equals zero, as shown in Fig. 3. Two other possible cases are investigated; they include impact angles of 30° and -30°. The resulting stresses due to the preceding cases are plotted in Fig. 4. The results in Fig. 4 correspond to a POD's body thickness of 1 mm, impact velocity of 7 km/h and impact Angle (IA) of 0°, 30° and -30°. The POD's body material used in the simulations is Steel 4340, with a Yield Strength (Y) of 470 MPa. In Fig. 4, it is noted that the most critical load is realized at IA= -30°. Therefore, all subsequent simulations will be done using this angle.

A. Impact Angle (IA)=0°

This case is shown in Fig. 3. As a result of the merging process, impact load will be distributed over the corresponding sides of the two PODs. Fig. 3 shows the directional deformation resulting from this load. In Fig. 4, it is shown that at an IA=0, the stress is generally minimum,

as compared to the other two cases. Therefore, no further investigation of this case is required. On the other hand, the behavior of the impact energy during the PODs attachment is shown in Fig. 5. It is shown that the internal energy increases during the impact then decreases afterwards, while the kinetic energy decreases during the impact then decrease afterwards. As for the hourglass and contact energies, they both stay constant during the impact.

TABLE I. MATERIAL PROPERTIES

No.	Material	Yield Strength (MPa)
1	Steel 4340	470
2	AL 1060-H12	61
3	Composite, Epoxy glass fiber	440
4	Plastic, ABS high impact	27.4

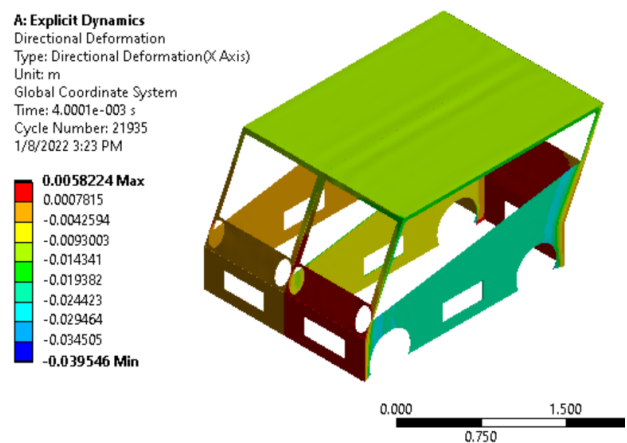


Figure 3. FEM model of the two merging PODs.

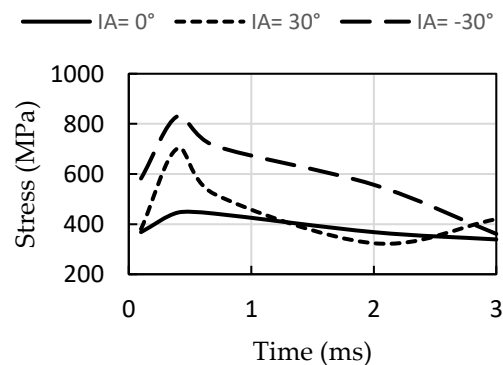


Figure 4. Stresses for different impact angles.

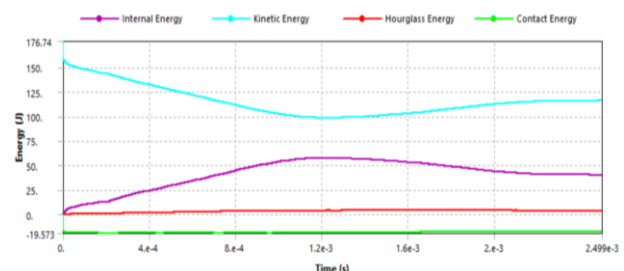


Figure 5. Impact energy during the PODs attachment.

B. Impact Angle (IA)=30°

This case is shown in Fig. 6 where the two PODs are in the process of merging, but due to certain condition such as wind, road level, navigational error, etc. at least one of them have shifted position. In this case an angle of 30° is assumed, where the first contact happens in the front part of the body side. As shown in Fig. 4, this case is generally more critical than the perfectly parallel PODs. However, it is clearly less critical than the case when IA= -30°. Therefore, the latter case will be pursued further.

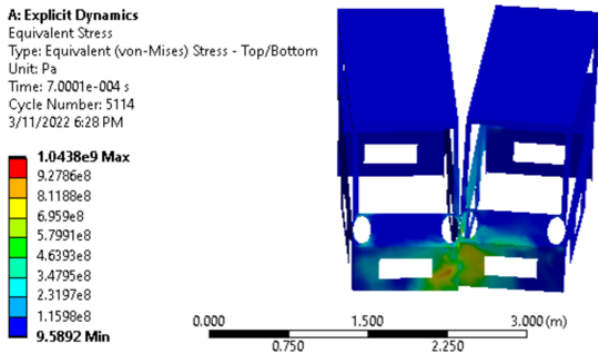


Figure 6. The two PODs merging at impact angle = 30°.

C. Impact Angle (IA)=-30°

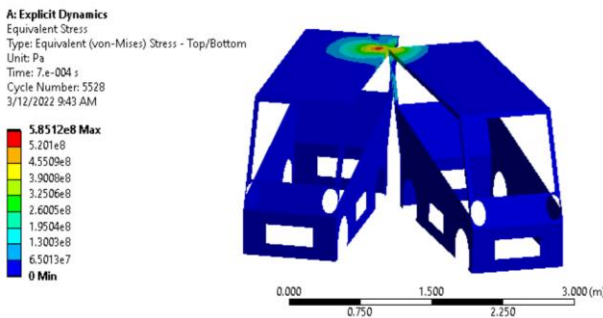


Figure 7. The two PODs merging at impact angle = -30°.

This case is shown in Fig. 7. As mentioned earlier, it is considered the most critical case because it results in the highest stress as shown in Fig. 4. For this case, acceleration versus time is plotted in Fig. 8. The POD's body thickness used in the analysis is 1 mm. the impact velocity is 8 km/h and the body material used is Steel 4340, with yield strength (Y) of 470 MPa. In Fig. 8, the deceleration shows a high value at the beginning of the impact, then it decreases later on. The deformation during the PODs' merging is shown in Fig. 9; the simulation conditions include; body thickness of 1 mm and impact velocity of 8 km/h. The body material used in this case is Steel 4340, with Yield strength (Y) of 470 MPa. It is noted that the deformation is faster at the beginning of the impact, then it slows down as the impact progresses.

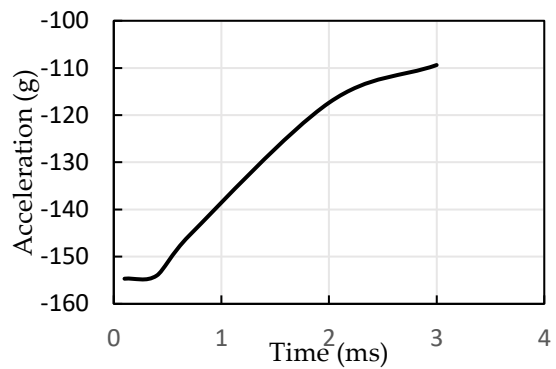


Figure 8. Acceleration during Pods' merging.

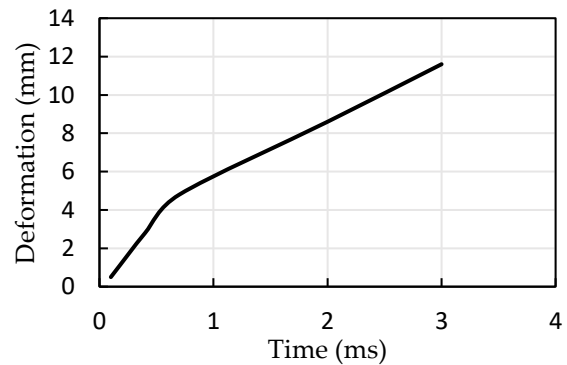


Figure 9. Deformation during Pods' merging.

The exerted force during the collision is shown in Fig. 10. The plot reflects the following conditions; body thickness of 1 mm and impact velocity of 8 km/h using Steel 4340 as the body material. It is noted that the force is maximum at the beginning of the impact. Fig. 11 shows the energy variation during the collision. The conditions include; body thickness of 1 mm and impact velocity of 8 km/h, using Steel 4340 as the body material. It is noted that the impact energy is highest at the beginning of the impact. The Stress- Strain curve of the impact is shown in Fig. 12. The tested body thickness is 1 mm made of Steel 4340 and the impact velocity is 8 km/h. The upper part of the curve represents loading and the lower part represents unloading, with less stress. It is noted that most of the strain bounces back, which means that the deformation is mostly elastic. Fig. 13 shows the variation of stress with impact velocity for steel 4340 with thickness of 1 mm. It is noted that the relationship is linear and proportional. The variation of equivalent stress with panel thickness is shown in Fig. 14; where the impact velocity is 8 km/h and the material is steel 4340. As expected, the relationship is proportional. Bearing in mind that the stress load is calculated based on Equivalent von Mises failure criterion, which is defined as [48]:

$$\sigma_0 = [\sigma_I^2 - \sigma_I \sigma_{II} + \sigma_{II}^2]^{1/2} \quad (3)$$

where σ_I and σ_{II} are the principal stresses. It is typical to see behaviors such as that shown in Fig. 15, and that is due to the changing values of the principal stresses in each loading scenario.

D. Other Body Panel Materials

So far, all the analyses have been conducted based on one material, which is steel 4340. However, there are other important materials which are increasingly being used for car body panels. In addition, some types of materials are investigated to check if they provide better performance than existing ones. The investigated body panel materials include AL 1060-H12 (Y=61 MPa), Composite, Epoxy glass fiber (Y=440 MPa) and Plastic, ABS high impact (Y=27.4 MPa). The results for these materials are presented in figures 15 to 21, based on an IA of -30° and body panel thickness of 1 mm; for AL 1060-H12, the stress variation with impact velocity is plotted in Fig. 15. It is noted that the curve is not linear as in the steel case. The variation of deformation with velocity is plotted in Fig. 16, where it exhibits a linear relationship. For composite, epoxy glass fiber, the variation of stress with velocity is shown in Fig. 17, which also exhibits a linear relationship. The variation of the deformation with velocity is shown in Fig. 18, which exhibits a linear relationship as well. Finally, for Plastic, ABS high impact, Fig. 19 shows the variation of stress with velocity and Fig. 20 shows the variation of deformation with velocity, where both figures exhibit linear relationships.

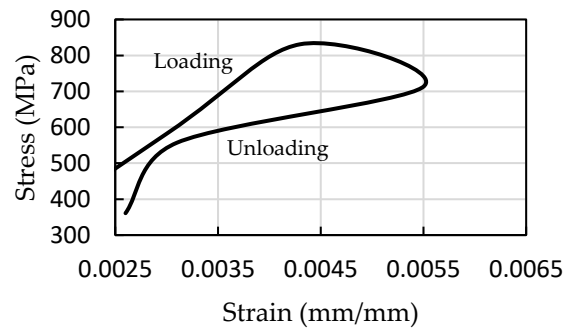


Figure 12. Stress vs. Strain (Steel 4340).

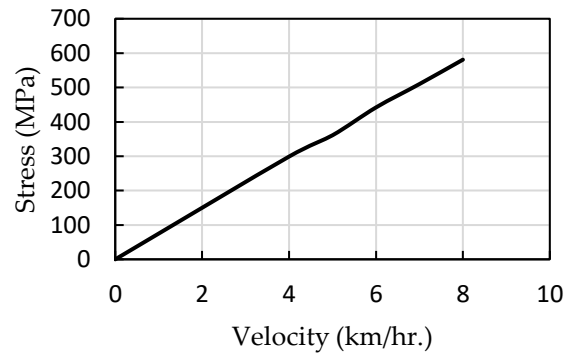


Figure 13. Stress vs. Impact Velocity (Steel 4340).

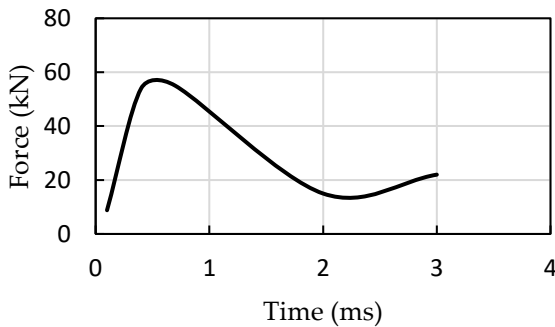


Figure 10. Force vs. Time (Steel 4340).

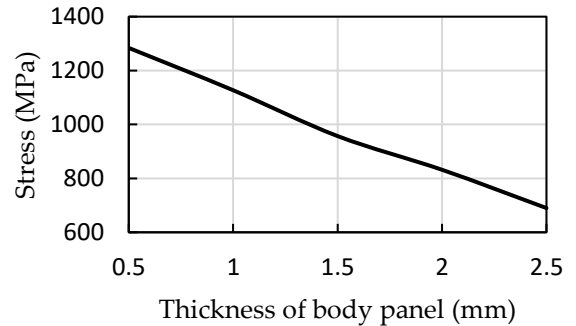


Figure 14. Stress vs. Thickness of body panel (Steel 4340).

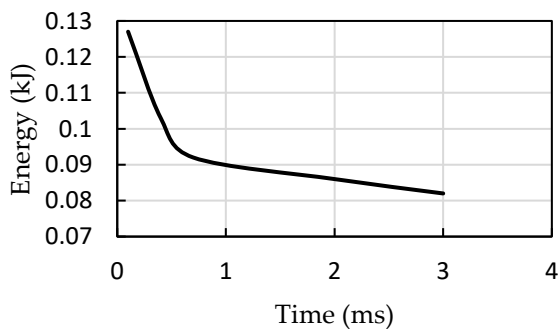


Figure 11. Energy vs. Time (Steel 4340).

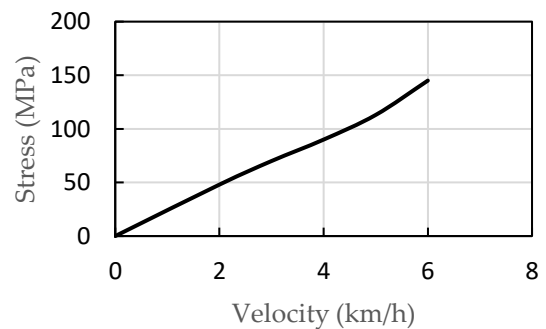


Figure 15. Stress vs. Impact velocity (AL 1060-H12).

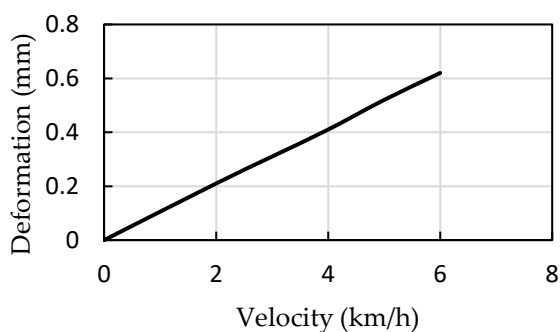


Figure 16. Deformation vs. Impact velocity (AL 1060-H12).

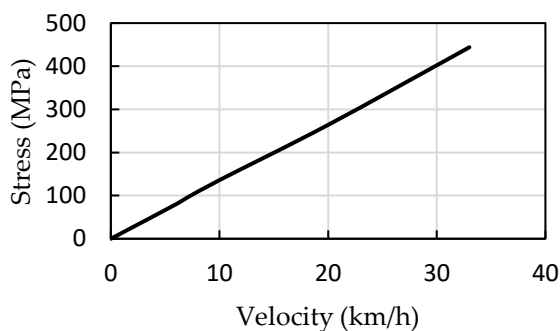


Figure 17. Stress vs. Impact velocity (Composite, epoxy glass fiber).

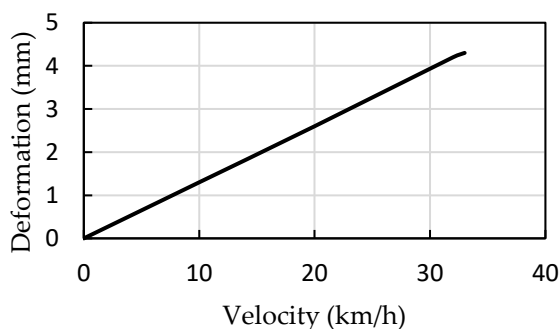


Figure 18. Deformation vs. Impact velocity (Composite, epoxy glass fiber).

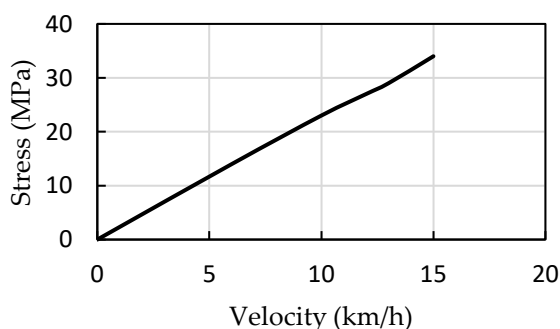


Figure 19. Stress vs. Impact velocity (Plastic, ABS high impact).

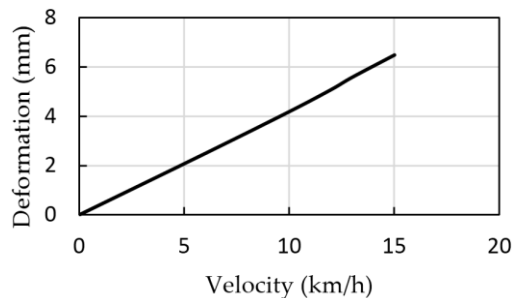


Figure 20. Deformation vs. Impact velocity (Plastic, ABS high impact).

The values of safe merging speeds for different body panel materials are shown in Table II and Fig. 21. The maximum safe merging speed can be obtained using Composite, Epoxy glass fiber as the body panel material, followed by Plastic, ABS high impact. As for the steel 4340, it comes in the third place. On the other hand, using AL 1060-H12 as the body panel material can only supports a merging speed of 2.5 km/h, which is the lowest in the list. Of course, additional materials can be investigated, as well as different alloys of the same metals, which may exhibit different behavior. It should be noted that it is not suggested here that composites or plastics are stronger than steel. Because the speeds that are tested are considered low and do not represent typical accidents. Beside the equivalent stress failure criteria that was employed in this work, other failure criteria for the body panel materials can be investigated, such as Hashin failure criteria [49], which states that Epoxy glass fiber composite can be damaged at an impact energy of 12 J. Moreover, Gohel et al. [50] reported that a 300 G acceleration can be considered a failure criteria for ABS high impact plastic. Furthermore, the effect of possible repetitive impacts on stiffness was studied by Kim and Cho [51].

TABLE II. MATERIAL PROPERTIES

No.	Body Panel Material	Safe Merging Speed (km/h)
1	Steel 4340	6
2	AL 1060-H12	2.5
3	Composite, Epoxy glass fiber	32
4	Plastic, ABS high impact	12

For validation purposes, the current results are compared with past results from the literature and good agreement was found, as shown in Table III. On the other hand, the effects of the different variables considered in this work on the PODs joining process are summarized in Table IV.

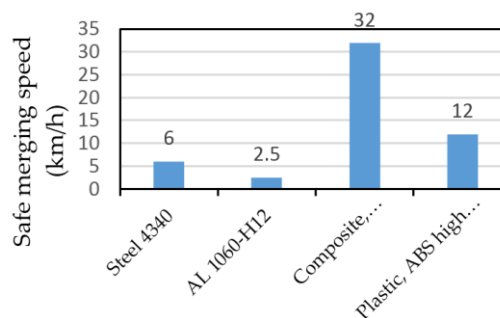


Figure 21. Safe PODs merging speeds for different body panel materials.

TABLE III. RESULTS VALIDATION

Material	Past Experiments/Unsafe Impact	This work/Safe Impact
Steel Alloy	Speed of 18 km/h [52]	Speed of 6 km/h
Aluminum Alloy	Load of 90 kN [53]	Load of 58 kN
Composite	Deformation of 27 mm [54]	Deformation of 4.5 mm
Plastic	Speed of 16 km/h [55]	Speed of 12 km/h

TABLE IV. VARIABLES EFFECTS ON THE JOINING PROCESS

Variable	Effect
Body material	The best material for this application is Composite, followed by Plastic, then Steel, while the worst is Aluminum.
Shell thickness	A higher thickness is better for this application. However, there must be a trade between cost and performance.
Impact speed	The speeds mentioned in Table II should not be exceeded.
Stress	All stresses should be maintained below the levels mentioned in Table I.
Deformation	Maximum deformation is noted in Plastic, followed by Composite, then Aluminum, and finally Steel.
Absorbed energy	The more energy absorbed, the safer the merging process. The best energy absorbent is Composite, followed by Plastic, then Steel, and the worst is Aluminum.

IV. CONCLUSIONS AND FUTURE WORK

The results indicate that it can be safe for two POD vehicles to merge together without causing any damage, even if the joining process was not perfect in terms of alignment. Due to the body design of the POD, the results showed that the most limiting misalignment angle during merger is -30, followed by 30, whereas perfect parallel docking results in the highest permitted joining speed. Therefore, to be on the conservative side, the most limiting angle of -30 is used for all subsequent simulations. Based on this fact, ceilings for merging speeds for different body panel materials have been suggested. These values can be elaborated further to cater for the exact need of a specific POD design and material. The use of epoxy glass fiber as the body panel material yielded the maximum allowable merging speed, followed by ABS high impact plastic. On the other hand, traditional metal alloys such as steel 4340 allowed less merging speeds, especially for AL 1060-H12 which showed intolerance to merging accidental impact. In general the procedure presented in this work has yielded reasonable results and can help to develop flexible autonomous transportation systems that can be adaptable to passengers' demand. As a recommendation for future work, alternative failure criteria for the body panel materials can be explored; for example, Epoxy glass fiber composites can be damaged at a certain level of impact energy. On the other hand, high values of acceleration can be used as a failure criteria for ABS high impact plastics. Furthermore, the effect of repetitive impacts on the vehicle strength may need further assessment.

CONFLICT OF INTEREST

The authors declare no conflict of interest.

AUTHORS CONTRIBUTIONS

Osama M. Al-Habahbeh conducted the research and drafted the manuscript; Romil S. Al-Adwan analyzed the data and did the formatting and editing. Both authors had approved the final version.

REFERENCES

- [1] X. He, Y. Liu, C. Lv, X. Ji, and Y. Liu, "Emergency steering control of autonomous vehicle for collision avoidance and stabilization," *Vehicle System Dynamics*, vol. 57, no. 8, pp. 1163-1187, 2019.
- [2] H. Xia, J. Chen, Z. Liu, and F. Lan, "Coordinated motion control for automated vehicles considering steering and driving force saturations," *Transactions of the Institute of Measurement and Control*, vol. 42, no. 1, pp. 157-166, 2020.
- [3] Prieve, "Vehicles for variably sized transportation," *US Patent* 10,882,575, Jan 5, 2021.
- [4] P. R. Williams, P. Kessler, and L. Herold, "Transportation system," *US Patent* 10359783B2, 2019.
- [5] Bick et al., "Vehicle combination and method for forming and operating a vehicle combination," *US Patent* 9,740,213, Aug 22, 2017.
- [6] Han et al., "Electronic docking vehicle," *US Patent* 9,914,495, Mar 13, 2018.
- [7] Evans, "Intelligent POD management and transport," *US Patent* 10,150,524, Dec 11, 2018.
- [8] Cervantes et al., "Road vehicle convoy control method, and road vehicle convoy," *US Patent* 10,538,240, Jan 21, 2020.
- [9] Wright, "Self-powered actively steerable converter dollies for long combination vehicles," *US Patent* 10,518,831, Dec 31, 2019.
- [10] C. Ulrich, H. E. Friedrich, J. Weimer, and S. A. Schmid, "New operating strategies for an on-the-road modular, electric and autonomous vehicle concept in urban transportation," *World Electric Vehicle Journal*, vol. 10, no. 91, 2019.
- [11] O. E. Gungor, R. She, I. L. Al-Qadi, and Y. Ouyang, "One for all: Decentralized optimization of lateral position of autonomous trucks in a platoon to improve roadway infrastructure sustainability," *Transportation Research Part C: Emerging Technologies*, vol. 120, Art. no. 102783, 2020.
- [12] S. Malik, P. Bandi, and W. Sun, "An experimental study of denial of service attack against platoon of smart vehicles," in *Proc. 4th International Conference on Connected and Autonomous Driving, MetroCAD*, Detroit, Apr. 2021, Code 171216, pp. 23-30.
- [13] N. A. Z. Abdullah, M. S. M. Sani, M. S. Salwani, and N. A. Husain, "A review on crashworthiness studies of crash box structure," *Thin-Walled Structures*, vol. 153, Art. no. 106795, 2020.
- [14] Q. Q. Li, E. Li, T. Chen, L. Wu, G. Q. Wang, and Z. C. He, "Improve the frontal crashworthiness of vehicle through the design of front rail," *Thin-Walled Structures*, vol. 162, Art. no. 107588, 2021.
- [15] X. Liu, R. Liang, Y. Hu, X. Tang, C. Bastien, and R. Zhang, "Collaborative optimization of vehicle crashworthiness under frontal impacts based on displacement oriented structure," *Int. J. Automotive Technology*, vol. 22, no. 5, pp. 1319-1335, 2021.
- [16] B. B. Munyazikwiye, D. Vysochinskiy, M. Khadyko, and K. G. Robbersmyr, "Prediction of vehicle crashworthiness parameters using piecewise lumped parameters and finite element models," *Designs*, vol. 2, no. 4, Art. no. 43, pp. 1-16, 2018.
- [17] L. Yu, X. Gu, L. Qian, P. Jiang, W. Wang, and M. Yu, "Application of tailor rolled blanks in optimum design of pure electric vehicle crashworthiness and lightweight," *Thin-Walled Structures*, vol. 161, Art. no. 107410, 2021.
- [18] I. Oztürk, N. Kaya, and F. Oztürk, "Design of vehicle parts under impact loading using a multi-objective design approach," *Materials Testing*, vol. 60, no. 5, pp. 501-509, 2018.
- [19] I. Saenz-Dominguez, I. Tena, A. Esnaola, M. Sarrionandia, J. Torre, and J. Aurrekoetxea, "Design and characterisation of cellular composite structures for automotive crash-boxes manufactured by out of die ultraviolet cured pultrusion," *Composites Part B: Engineering*, vol. 160, pp. 217-224, 2019.
- [20] Y. Chen, X. Cheng, and K. Fu, "Multi-material design of a vehicle body considering crashworthiness safety and social effects," *Int. J. Crashworthiness*, vol. 25, no. 5, pp. 517-526, 2020.

- [21] N. S. B. Yusof, S. M. Sapuan, M. T. H. Sultan, and M. Jawaid, "Conceptual design of oil palm fibre reinforced polymer hybrid composite automotive crash box using integrated approach," *J. Central South University*, vol. 27, no. 1, pp. 64-75, 2020.
- [22] X. Jin, H. Hou, M. Shen, H. Wu, and K. H. Yang, "Occupant kinematics and biomechanics with rotatable seat in autonomous vehicle collision: A preliminary concept and strategy," in *Proc. Conf. Proc. International Research Council on the Biomechanics of Injury, IRCOBI*, Athens, Sep. 2018, Code 143981, pp. 106-113.
- [23] Q. Chen, Y. Xie, Y. Ao, T. Li, G. Chen, S. Ren, C. Wang, and S. Li, "A deep neural network inverse solution to recover pre-crash impact data of car collisions," *Transportation Research Part C: Emerging Technologies*, vol. 126, Art. no. 103009, 2021.
- [24] Q. Liu, H. Shen, Y. Wu, Z. Xia, J. Fang, and Q. Li, "Crash responses under multiple impacts and residual properties of CFRP and aluminum tubes," *Composite Structures*, vol. 194, pp. 87-103, 2018.
- [25] I. Öztürk, N. Kaya, and F. Öztürk, "Effects of material failure criteria on design of vehicle parts under impact loading," *Int. J. Crashworthiness*, 2020.
- [26] F. Zong, M. Wang, J. Tang, and M. Zeng, "Modeling AVs & RVs' car-following behavior by considering impacts of multiple surrounding vehicles and driving characteristics," *Physica A: Statistical Mechanics and its Applications*, vol. 5891, Art. no. 126625, 2022.
- [27] K. Lee and D. Kum, "Collision avoidance/mitigation system: Motion planning of autonomous vehicle via predictive occupancy map," *IEEE Access*, vol. 7, Art. no. 8698763, pp. 52846-52857, 2019.
- [28] Y. Song, M. V. Chitturi, and D. A. Noyce, "Automated vehicle crash sequences: Patterns and potential uses in safety testing," *Accident Analysis and Prevention*, vol. 153, Art. no. 106017, 2021.
- [29] C. Xu, Z. Ding, C. Wang, and Z. Li, "Statistical analysis of the patterns and characteristics of connected and autonomous vehicle involved crashes," *J. Safety Research*, vol. 71, pp. 41-47, 2019.
- [30] A. Corso, P. Du, K. Driggs-Campbell, and M. J. Kochenderfer, "Adaptive stress testing with reward augmentation for autonomous vehicle validation," *IEEE Intelligent Transportation Systems Conference ITSC*, Auckland, Oct. 2019, Art. no. 8917242, pp. 163-168.
- [31] H. Chen, R. Zhou, Z. Liu, and X. Sun, "Exploring the mechanism of crashes with AV using machine learning," *Mathematical Problems in Engineering*, Art. no. 5524356, 2021.
- [32] C. L. Walker, B. Boyce, C. P. Albrecht, and A. Siems-Anderson, "Will weather dampen self-driving vehicles?" *Bulletin of the American Meteorological Society*, vol. 101, no. 11, pp. E1914-E1923, 2020.
- [33] M. Dlugosch, J. Fritsch, D. Lukaszewicz, and S. Hiermaier, "Experimental investigation and evaluation of numerical modeling approaches for hybrid-FRP-steel sections under impact loading for the application in automotive crash-structures," *Composite Structures*, vol. 174, pp. 338-347, 2017.
- [34] U. Müller, T. Jost, C. Kurzböck, A. Stadlmann, W. Wagner, S. Kirschbichler, G. Baumann, M. Pramreiter, and F. Feist, "Crash simulation of wood and composite wood for future automotive engineering," *Wood Material Science and Engineering*, vol. 15, no. 5, 2020.
- [35] X. Liu, X. Qu, and X. Ma, "Improving flex-route transit services with modular autonomous vehicles," *Transportation Research Part E: Logistics and Transportation Review*, vol. 149, 102331, 2021.
- [36] X. Liu, X. Ma, and Z. Liu, "Scheduling optimization of electric self-driving modular vehicles for public transportation," *Chinese Journal of Highways*, vol. 35, no. 3, 2022.
- [37] M. Chinmay, F. Hua, W. Honggang, and Y. Qing, "Adaptive vehicle platooning with joint network-traffic approach," *IEEE Global Communications Conference, GLOBECOM-Proceedings*, Madrid, 7-11 Dec. 2021, Code 176805.
- [38] Q. Tian, Y. H. Lin, D. Z. W. Wang, and Y. Liu, "Planning for modular-vehicle transit service system: Model formulation and solution methods," *Transportation Research Part C: Emerging Technologies*, vol. 138, 103627, 2022.
- [39] R. Lamotte, A. Palma, and N. Geroliminis, "On the use of reservation-based autonomous vehicles for demand management," *Transportation Research Part B: Methodological*, vol. 99, pp. 205-227, 2017.
- [40] Y. Ji, B. Liu, Y. Shen, and Y. Du, "Scheduling strategy for transit routes with modular autonomous vehicles," *International Journal of Transportation Science and Technology*, vol. 10, no. 2, pp. 121-135, 2021.
- [41] Z. Chen, X. Li, and X. Zhou, "Operational design for shuttle systems with modular vehicles under oversaturated traffic: Continuous modeling method," *Transportation Research Part B: Methodological*, vol. 132, pp. 76-100, 2020.
- [42] X. Shi, Z. Chen, M. Pei, and X. Li, "Variable-capacity operations with modular transits for shared-use corridors," *Transportation Research Record*, vol. 2674, no. 9, pp. 230-244, 2020.
- [43] X. Liu, X. Ma, and Z. Liu, "Dispatch optimization of electric autonomous modular vehicles for public transport," *Zhongguo Gonglu Xuebao/China Journal of Highway and Transport*, vol. 35, no. 3, pp. 240-248, 2022.
- [44] M. Tholen, B. A. Beirigo, J. Jovanova, and F. Schulte, "The share-A-Ride problem with integrated routing and design decisions: The case of mixed-purpose shared autonomous vehicles," *Lecture Notes in Computer Science*, vol. 13004, LNCS, pp. 347-361, 2021.
- [45] A. Fielbaum, "Strategic public transport design using autonomous vehicles and other new technologies," *Int. J. ITS Res.*, vol. 18, pp. 183-191, 2020.
- [46] M. Pei, P. Lin, J. Du, X. Li, and Z. Chen, "Vehicle dispatching in modular transit networks: A mixed-integer nonlinear programming model," *Transportation Research Part E: Logistics and Transportation Review*, vol. 147, Art. no. 102240, 2021.
- [47] R. C. Hibbeler, *Engineering Mechanics- Dynamics*, 14th ed., New Jersey 07030, USA: Pearson Prentice Hall, 2016.
- [48] F. A. Leckie and D. J. Dal Bello, *Strength and Stiffness of Engineering Systems, Mechanical Engineering Series*, NY 10013, USA: Springer Science, 2009.
- [49] N. A. Nassir and M. R. Gharkan, "Impact response of composite laminates based on epoxy and glass fibre," in *Proc. 3rd International Conference on Materials Engineering & Science, Material Today: Proceedings*, vol. 42, part 5, pp. 1901-1907, 2021.
- [50] G. Gohel, S. K. Bhudolia, S. B. S. Elisetty, K. F. Leong, and P. Gerard, "Development and impact characterization of acrylic thermoplastic composite bicycle helmet shell with improved safety and performance," *Composite Part B*, vol. 221, 2021.
- [51] S. Kim and H. Cho, "Interpretation of stiffness change over the trunk side of a vehicle upon a re-accident after repair its former rear impact collision accident," *International Journal of Mechanical Engineering and Robotics Research*, vol. 10, no. 7, pp. 406-413, 2021.
- [52] A. T. Zehnder and A. J. Rosakis, "Dynamic fracture initiation and propagation in 4340 steel under impact loading," *International Journal of Fracture*, vol. 43, no. 4, pp. 271-285, 1990.
- [53] C. Chen, H. Zhang, X. Ren, and J. Wu, "Investigation of flat-clinching process using various thicknesses aluminum alloy sheets," *International Journal of Advanced Manufacturing Technology*, vol. 114, no. 7-8, pp. 2075-2084, 2021.
- [54] Y. Chen, X. Zeng, Y. Deng, and G. Wei, "Investigation on manufacturing and low-velocity impact performance of all-composite sandwich structure with S-type foldcore," *Composite Structures*, vol. 29015, Art. no. 115539, 2022.
- [55] X. Wang, X. Tang, X. Hu, and P. Wang, "Dynamic tensile mechanical behavior of polyurethane films incorporated with functionalized graphene oxide," *Polymer*, vol. 24619, Art. no. 124755, 2022.

Copyright © 2022 by the authors. This is an open access article distributed under the Creative Commons Attribution License (CC BY-NC-ND 4.0), which permits use, distribution and reproduction in any medium, provided that the article is properly cited, the use is non-commercial and no modifications or adaptations are made.



Osama M. Al-Hababbeh is an Associate Professor and Head of the Mechatronics Engineering Department at the University of Jordan. He earned his PhD in Mechanical Engineering from Clarkson University at New York. He was a Deputy Dean of students' Affairs and Director of Career Guidance and Alumni Office. He published 2 books and 40 Journal and conference papers. His research interests include reliability, energy, and autonomous systems. Dr. Al-Hababbeh has long years of experience in aerospace, manufacturing, tourism, and academia. He held technical and leading positions at different

organizations in Jordan, Malaysia, Australia, Kuwait, and United States. Currently, he provides consulting for reputable regional clients.



Romil S. Al-Adwan earned his PhD in Mechanical Engineering from the University of Northumbria at Newcastle, UK. He is currently teaching at the department of mechatronics engineering, at the University of Jordan. He also taught several industrial and mechanical engineering courses, at different universities. Dr. Al-Adwan has more than 30 years of experience in various sectors including defense, telecom, manufacturing,

and academia. He held technical and managerial positions at different international organizations in Jordan, Canada, Hong Kong, and United States.